Ion Diffusion within Charged Porous Network as Probed by Nuclear Quadrupolar Relaxation

Alfred Delville,* Patrice Porion, and Anne Marie Faugère

CRMD, CNRS, 1B rue de la Férollerie, 45071 Orléans Cedex 02, France

Received: September 1, 1999; In Final Form: December 2, 1999

^{23}Na and ^{7}Li relaxation measurements were used over a broad range of frequencies to determine ion diffusion in aqueous dispersions of Montmorillonite and Laponite clays. In agreement with our previous Brownian dynamics simulations of ion diffusion and relaxation in such heterogeneous system, the spectral densities of these $^{3}/_{2}$ spin nuclei exhibit a transition between two dynamical regimes characterized by a plateau and a power-law decrease. The frequency crossover is determined by the spatial extent of microdomains composed of partially oriented clay particles. This result illustrates the potentiality of nuclear quadrupolar relaxation as a sensitive probe of the spatial propagation of orientational order within heterogeneous systems limited by charged interfaces.

I. Introduction

Nuclear quadrupolar relaxation of ^{23}Na and ^{7}Li is used in order to investigate ion mobility within the porous network existing in aqueous dispersions of clay particles. Suspensions of these highly anisotropic charged particles are used in many industrial applications (drilling, cosmetic and food industry, waste management, etc.) because of their various physicochemical properties (thixotropy, swelling, gelling, ionic exchange capacity, adsorption, etc.). The long-range electrostatic coupling between these charged colloids is responsible for their structural and dynamical properties.[1,2] Since it is modulated by their ionic diffuse layer,[1,2] we used nuclear quadrupolar relaxation (NQR) to derive dynamical information on the neutralizing counterions.

The systems under study are dispersions of synthetic (Laponite) and natural (Montmorillonite) clays in dilute (10^{-2} M) solutions of sodium or lithium chloride. These clays, which have nearly the same surface charge density ($\sigma \approx 7 \times 10^{-3}$ e/Å^2), are neutralized by sodium counterions and differ mainly by their size: synthetic Laponite (the smallest) is characterized[3] by a lateral extent of 300 Å, and Montmorillonite extends laterally[4] up to 10^4 Å. However, because of the flexibility of the aluminosilicate layers, the order of magnitude of the persistence length of sodium Montmorillonite, as probed by electronic microscopy,[5] is about 4000 Å.

Previous ^{23}Na NQR investigations on heterogeneous systems showed the efficiency of NQR as a probe of the dynamical properties of the sodium counterions.[6−9] Furthermore, our multiscale analysis of the diffusion and relaxation of quadrupolar nuclei within clay suspensions suggested[9] the potentiality of NQR as a probe of the spatial extent of orientational correlations between the directors of charged interfaces.

We thus performed NQR of different quadrupolar nuclei (^{23}Na and ^{7}Li) in the presence of charged lamellar colloids of various size to test this conjecture. These relaxation measurements confirm the existence of two dynamical regimes characterized by a plateau and a power-law decrease of the spectral densities, as predicted by our preliminary study.[9] Furthermore, the crossover frequency is related to the spatial extent of the microdomains composed by partially oriented clay particles. However, the agreement between theoretical and experimental results is only semiquantitative, because our predictions significantly overestimate the slope detected in the high frequency domain of the spectral densities.

II. Materials and Methods

(A) Clay Dispersions. Laponite RD (Laporte) was used without further treatment. Laponite clays are lamellae resulting from the sandwiching of one layer of octahedral magnesium oxides (three per unit cell) between two tetrahedral silica layers. Some Mg atoms of the octahedral network are replaced by lithium, leading to negative charges on the clay particle. These charges are neutralized by exchangeable sodium counterions.

The natural Montmorillonite clay (Wyoming) has a different chemical composition: its octahedral network is aluminum oxide layers (two per unit cell). Here also, octahedral substitution of aluminum by magnesium or iron is mainly responsible for the negative charge of the clay network. Some additional charges result from substitution of silicon of the tetrahedral network by aluminum.[10] This natural clay is purified by standard procedures:[4] centrifugation, ionic exchange, and dialysis against pure water. All clays are dispersed in sodium hydroxide (10^{-4} M) to prevent dissolution of the magnesium oxide from the octahedral network of Laponite.[11]

(B) NMR Measurements. Spectra were recorded on DSX360, MSL200, and DSX100 Bruker spectrometers at fields of 8.465, 4.702, and 2.351 T, respectively (superconducting magnets). On these spectrometers, the pulse durations for total inversion of the longitudinal magnetization of ^{23}Na and ^{7}Li vary between 4 and 12 μs. Spectra from the DSX360 and DSX100 spectrometers were recorded using a fast acquisition mode with a time step of 1 μs, corresponding to a spectral width of 1 MHz. The dead time of both these spectrometers plus the time delay before recording the transverse magnetization was 5 μs, allowing the acquisition of the fast and slow components of the transverse magnetization. Spectra from the MSL200 spectrometer were recorded using a slower acquisition mode with a time step varying between 10 and 50 μs, corresponding to spectral widths of 100 and 20 kHz respectively. Because of the longer delay before acquisition on this spectrometer, we detected only the

10.1021/jp993107l CCC: $19.00
Published on Web 02/01/2000

slow component of the transverse magnetization. ^{7}Li spectra in the presence of clay were recorded using a time delay of a few seconds between each pulse in order to recover the total longitudinal magnetization. Longitudinal relaxation rates were measured according to the classical $180-\tau-90$ pulse sequence, while Hahn echoes were used to measure the transverse relaxation rates. Longitudinal relaxation rates in the rotating frame were measured on the DSX360 spectrometer after calibration of the transverse field.

(C) Relaxation of $^3/_2$ Spin Nuclei under Slow Modulation. The quadrupolar Hamiltonian may be written as[12-15]

$$H_Q(\tau) = C_Q \sum_{m=-2}^{2} (-1)^m F_{-m}(t)\, A_m(I) \tag{1}$$

where $C_Q = (eQ)/(2I(2I-1)\hbar)$, $-e$ is the electron charge and Q the quadrupolar moment of the nucleus (0.11×10^{-28} m^2 for ^{23}Na and -0.04×10^{-28} m^2 for ^{7}Li).[16] The $A_m(I)$ factors in eq 1 are spin operators:

$$A_0 = 1/\sqrt{6}(3I_z^2 - I(I+1)) \tag{2a}$$

$$A_{\pm 1} = \pm 0.5(I_z I_\pm + I_\pm I_z) \tag{2b}$$

$$A_{\pm 2} = 0.5 I_\pm^2 \tag{2c}$$

The $F_m(\tau)$ factors are derived from instantaneous components of the electric field gradient (efg) tensor expressed in a laboratory frame (with the z axis parallel to the magnetic field):

$$F_0 = (1.5)^{1/2} V_{zz}^{\,D}(1+\gamma_\infty) Y_0^{\,DL} \tag{3a}$$

$$F_{\pm 1} = \pm (V_{xz}^{\,D} \pm i V_{yz}^{\,D})(1+\gamma_\infty) Y_{\pm 1}^{\,DL} \tag{3b}$$

$$F_{\pm 2} = 0.5(V_{xx}^{\,D} - V_{yy}^{\,D} \pm 2i V_{xy}^{\,D})(1+\gamma_\infty) Y_{\pm 2}^{\,DL} \tag{3c}$$

where $(1+\gamma_\infty)$ is the Sternheimer antishielding factor resulting from the polarization of the innermost electronic orbital of the nucleus by the external source of efg.[17]

The instantaneous components of the efg tensor ($V_{\alpha\beta}^{D}(\tau)$) are generally evaluated in a frame fixed to the probing nucleus. Spherical harmonics of rank 2 use Euler angles to describe the orientation of this instantaneous local frame within the laboratory frame:[12,13]

$$Y_0^{\,DL} = (5/16\pi)^{1/2}(3\cos^2\theta(\tau) - 1) \tag{4a}$$

$$Y_{\pm 1}^{\,DL} = (15/8\pi)^{1/2} \sin\theta(\tau)\cos\theta(\tau)\exp(\pm i\phi(\tau)) \tag{4b}$$

$$Y_{\pm 2}^{\,DL} = (15/32\pi)^{1/2} \sin^2\theta(\tau)\exp(\pm 2i\phi(\tau)) \tag{4c}$$

The transverse and longitudinal magnetization of $^3/_2$ spin nucleus is the sum of two components, with a priori known relative abundance:[18-22]

$$M_x(t) = M_x(0)[0.4\exp(-t/T_2^{\,s}) + 0.6\exp(-t/T_2^{\,f})] \tag{5a}$$

$$M_z(t) - M_z(\infty) = 2M_z(0)[0.8\exp(-t/T_1^{\,s}) + 0.2\exp(-t/T_1^{\,f})] \tag{5b}$$

The relaxation rates ($R_i^\alpha = 1/T_i^\alpha$, $i = 1, 2$, $\alpha =$ f, s) are linear combinations of the spectral densities [$J_m(\omega)$], which are Fourier transforms of the autocorrelation functions of the time fluctuating components $F_m(\tau)$ of the quadrupolar Hamiltonian (eq 3):

$$R_2^{\,f} = 3C_Q^{\,2}[J_0(0) + J_1(\omega_0)] \tag{6a}$$

$$R_2^{\,s} = 3C_Q^{\,2}[J_1(\omega_0) + J_2(2\omega_0)] \tag{6b}$$

$$R_1^{\,f} = 6C_Q^{\,2} J_1(\omega_0) \tag{6c}$$

$$R_1^{\,s} = 6C_Q^{\,2} J_2(2\omega_0) \tag{6d}$$

$$J_m(\omega) = FT[\langle F_m(0) F_{-m}(\tau)\rangle] \tag{6e}$$

By transforming the quadrupolar Hamiltonian expressed in the laboratory frame (eqs 1-3) into the double rotating tilted frame,[23] we derived expressions of $T_{1\rho}$ for $^3/_2$ nuclei under conditions of slow modulation:

$$M^1{}_z(t) = M^1{}_z(0)[0.8\exp(-t/T_{1\rho}^{\,f}) + 0.2\exp(-t/T_{1\rho}^{\,s})] \tag{7}$$

where

$$R_{1\rho}^{\,f} = {}^3/_4 C_Q^{\,2}[3J_0(2\omega_1) + 4J_1(\omega_0) + J_2(2\omega_0)] \tag{8a}$$

$$R_{1\rho}^{\,s} = 3C_Q^{\,2}[J_1(\omega_0) + J_2(2\omega_0)] \tag{8b}$$

III. Results and Discussion

(A) ^{23}Na Relaxation in Laponite Dispersions. ^{23}Na relaxation measurements of aqueous dispersions of clays neutralized by sodium counterions showed[9] the coexistence of two transverse relaxation rates (Figure 1a), while free and condensed counterions exchange rapidly on the NMR time scale (faster than 10^{-3} s^{-1}). This behavior results from the slow modulation of the residual quadrupolar coupling felt by sodium counterions condensed at the surface of the clay particles. By contrast with the theoretical predictions (cf. eq 5), a single component of the longitudinal magnetization is detected (Figure 1b) since the two contributions ($R_1^{\,f}$ and $R_1^{\,s}$) are too similar to be distinguishable (cf eqs 6c and d).

In order to interpret these data, we developed[9] a multiscale analysis of ion diffusion and relaxation within heterogeneous systems. We first used a molecular description of the clay/water interface[24,25] in order to describe the structure of the hydration layers[1] at contact with the clay surface (i.e., within an elementary cube of 30 Å side). At a larger scale (2000 Å), we used the primitive model to determine the fraction of counterions condensed[32,33] at the vicinity of a single clay particle. Finally, at a very large scale (10000 Å), we simulated the distribution of hard discs to generate a porous media in which ion diffusion will occur. The thickness of each hard disc[9] was set to 30 Å, i.e., the size of the elementary cell used in our molecular description of the clay/water interface (see above). We used such an elementary volume in order to include the three layers of strongly structured water molecules located on both sides of the clay particle, with an apparent thickness less than 10 Å.

This molecular description of the clay/water interface[24,25] was the starting point of our analysis, by predicting a nonzero residual quadrupolar coupling (V_{zz}^{static})[9] for the sodium counterions near the clay surface (at separation smaller than 15 Å). The principal axis of the tensor characterizing their quadrupolar coupling was found to be aligned along the clay director.

Numerical simulations of Brownian dynamics were then performed[9] to describe the diffusion of sodium ions within the porous network limited by the clay surfaces. We neglected ion/ion and ion/clay interactions and assumed an average residence

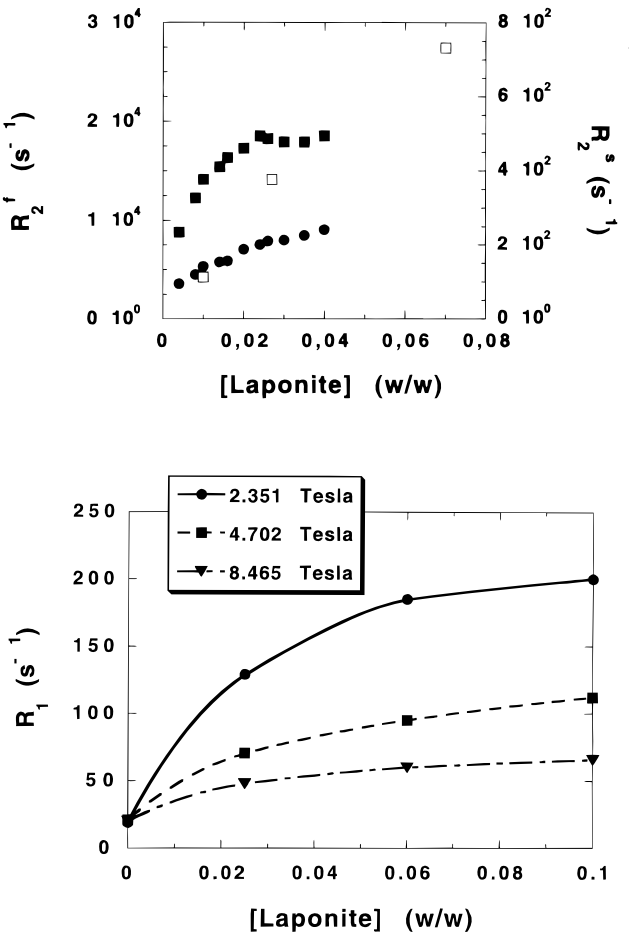

Figure 1. Influence of the Laponite concentration: (a) on the two components of the ^{23}Na transverse relaxation rate measured at 8.465 Tesla (black squares, experimental R_2^f; black dots, experimental R_2^s; white squares, theoretical R_2^f); and (b) on the ^{23}Na longitudinal relaxation rate measured at three field strengths.

time of 1 ns for the sodium counterions located within a cylinder of 30 Å thickness centered around each clay particle. A simple two-step model was then used to describe the quadrupolar coupling felt by sodium counterions diffusing within the clay dispersion: either zero in the bulk phase or the residual static value during its residence in the neighboring of one clay particle[9] (see above). In that context, initially condensed counterions loose the memory of the orientation of their host clay particle by diffusing through the clay network, probing the spatial extent of locally ordered microdomains:

$$G_Q(\tau) = \langle F_0^{\text{static}}(0) F_0^{\text{static}}(\tau)\rangle = \frac{15\,(V_{zz}^{\text{static}}\,(1+\gamma_\infty))^2}{32\pi \text{Nat}} \{\sum_{i=1}^{\text{Nat}}\sum_{j=1}^{\text{Npt}}\sum_{k=1}^{\text{Npt}} p(i\in j|0)\,p(i\in k|\tau)(3\cos^2\theta_j - 1)\,(3\cos^2\theta_k - 1)\} \quad (9)$$

where Nat and Npt are respectively the total number of counterions and clay particles and $p(i\in k|\tau)$ is the probability of finding ion i condensed on particle k at time τ. This model ignores the contribution of fast relaxation mechanisms, but reproduced[9] the order of magnitude of the fast component of the ^{23}Na transverse relaxation rates in presence of Laponite clay (see Figure 1a).

As shown on Figure 1a and b, the longitudinal relaxation rate and the two components of the transverse relaxation rate increase as a function of the clay concentration. These results

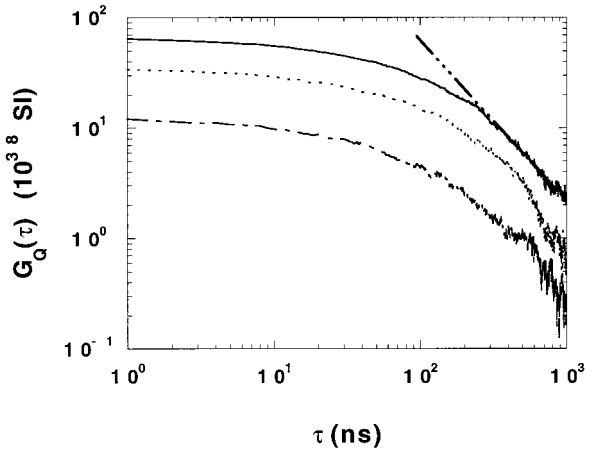

Figure 2. Correlation function of ^{23}Na quadrupolar coupling as calculated from Brownian simulations of ion diffusion within model of Laponite dispersions (−, 7%; − −, 2.7%, and −•−, 1%).

are well reproduced by a fast exchange regime between two different environments corresponding respectively to free and condensed[32,33] counterions:

$$R_i^{\alpha} = P_F R_i^{\alpha}{}_F + p_C R_i^{\alpha}{}_C \quad (10)$$

As the clay concentration increases, the fraction of condensed counterions increases almost linearly, because the amount of counterions condensed on a single clay particle is nearly independent of the clay concentration.[32,33] However, the relaxation rates of these condensed counterions is a decreasing function of the clay concentration, because of the corresponding decrease of the average separation between the clay particles. As a consequence, initially condensed counterions have to diffuse during a shorter time to reach another clay particle with a different orientation if the clay concentration is higher. The same behavior was already reported for relaxation measurements of sodium counterions in presence of cylindrical polyions.[38,39] The final balance between these two effects is a gradual saturation of the increase of the sodium relaxation rates as a function of the clay concentration, as displayed in Figure 1a and b.

As shown in Figure 2, initially condensed counterions keep the memory of their quadrupolar coupling for a time scale (10^{-7} s) two orders of magnitude larger then their average residence time ($\tau_B \sim 10^{-9}$ s). Assuming a diffusion coefficient of 10^{-5} cm^2/s, this time corresponds to the diffusion through a domain of 100 Å, i.e., of the same size than the ordered microdomains generated by the small Laponite particles (Figure 3). At longer times, the memory function of the quadrupolar coupling evolves (Figure 2) according to a power law ($\tau^{-3/2}$), as expected for relaxation induced by diffusion in an isotropic 3D space.[26,27] As a consequence, the long-time memories of the quadrupolar coupling and the crossover displayed in Figure 2 are governed by the propagation of the local nematic order of the clay particles within the suspension. The resulting spectral densities shown on Figure 4 display two well-separated frequency regimes: (i) at high frequency, a power law decrease ($J(\omega) \sim \omega^{-1.5\pm0.5}$), corresponding to diffusion within ordered microdomains, and (ii) at low frequency, a classical variation ($J(\omega) = a - b\sqrt{\omega}$), corresponding to diffusion within an isotropic 3D space.[26,27]

The crossover between these two different regimes was predicted to occur, for Laponite suspensions, at $\omega \sim (2-4) \times 10^6$ s^{-1}. The large difference between the fast and slow components of the transverse relaxation rates is the consequence of this frequency variation of the ^{23}Na spectral densities.

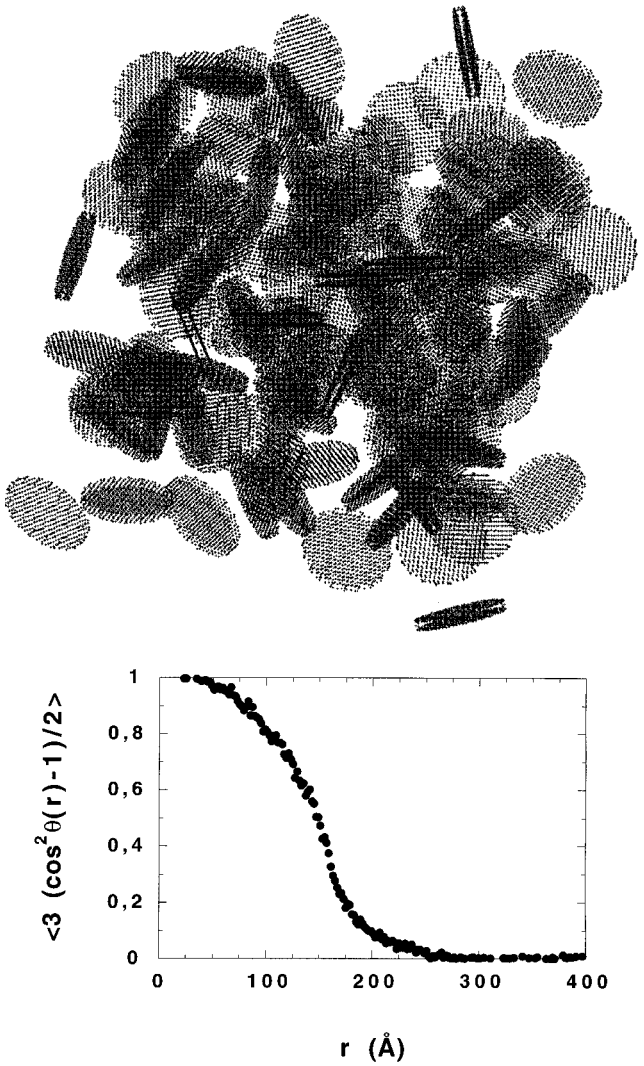

Figure 3. Model of Laponite dispersion used in the dynamical simulations (a) and the resulting local order parameter characterizing the spatial extent of oriented microdomains (b).

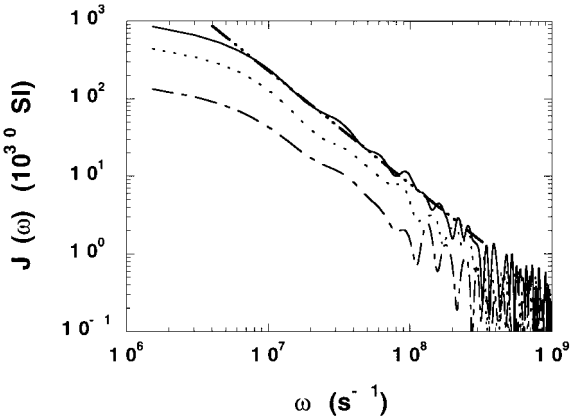

Figure 4. Theoretical spectral densities obtained by Fourier transform of the autocorrelation functions shown on Figure 2 (same labels as those in Figure 2).

In order to check the validity of this analysis, we performed relaxation measurements at various frequencies, including relaxation measurements under spin-locking conditions to investigate a broad range of frequencies. Such experiments were already performed to analyze dipolar and quadrupolar relaxation of molecular probes confined within porous media.[26−31] Note that, because of the order of magnitude of the ^{23}Na longitudinal relaxation rates ($T_1 \sim 10^{-3}$ s), field cycling[28−29] appears to be useless because of the time required to switch the magnitude of the magnetic field. As already shown on Figure 1b, ^{23}Na relaxation rate in presence of Laponite clay is very sensitive to the field strength. The frequency variations of T_1 and $T_{1\rho}$ reported on Figure 5 are in semiquantitative agreement with the predictions of Figure 4. The crossover occurs at the same frequency but the high-frequency power-law variation displayed on Figure 5 ($J(\omega) \sim \omega^{-0.9\pm0.1}$) differs somewhat from the predicted one ($J(\omega) \sim \omega^{-1.5\pm0.5}$, see Figure 4). Despite the experimental and theoretical power-law variations of the spectral densities ($J(\omega)$) have the same order of magnitude, they correspond to completely different time variation of the correlation function of the quadrupolar coupling ($G_Q(\tau)$). The experimental data correspond to a logarithmic variation:

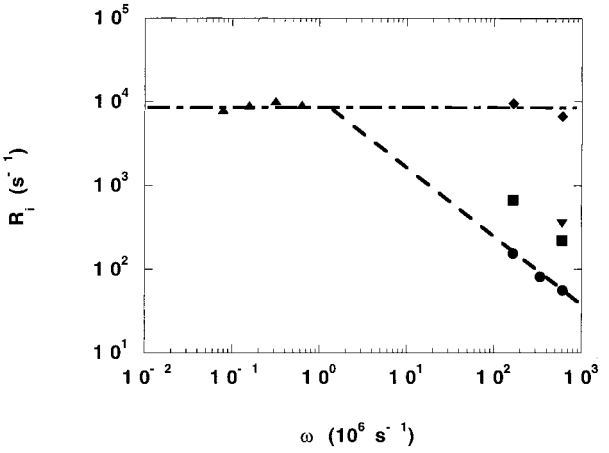

Figure 5. Frequency variation of ^{23}Na relaxation rates measured for aqueous suspensions of Laponite (5%, w/w): (●, R_1; ◆, R_2^f; ■, R_2^s; ▲, $R_{1\rho}^f$; ▼, $R_{1\rho}^s$).

$$G_Q(\tau) = (A - B)\ln(\tau) \tag{11}$$

while our model predicts a square root dependence:

$$G_Q(\tau) = (A - B)\sqrt{(\tau)} \tag{12}$$

for a time period smaller than 200 ps, corresponding to the time limit at which the asymptotic decrease of $G_Q(\tau)$ occurs (cf. Figure 2).

This discrepancy results from the numerous approximation used in our model: first, we assume the coexistence of only two limiting environments, characterizing respectively free and condensed counterions; secondly, we confine the condensed counterions in a small shell of constant thickness (∼10 Å) centered on the clay particle; thirdly, we perform simple simulations of Brownian Dynamics and neglect any ion/ion or clay/ion interactions in the calculation of the trajectories of the free ions during their diffusion through the porous network limited by the charged clay particles; fourthly, we freeze the motion of the counterions condensed at the surface of the clay particle; and finally, we neglect the contribution of the electric field gradient felt by the free counterions in the derivation of the autocorrelation function of their quadrupolar coupling.

As a consequence, the agreement between experimental and theoretical data is only semiquantitative, and a better agreement should be obtained by performing full Molecular Dynamics simulations, including the exact electrostatic force field felt by condensed and free counterions. In addition to condensation and interionic correlation effects,[32,33] this treatment will include the contribution from the long-range electric field felt by the free

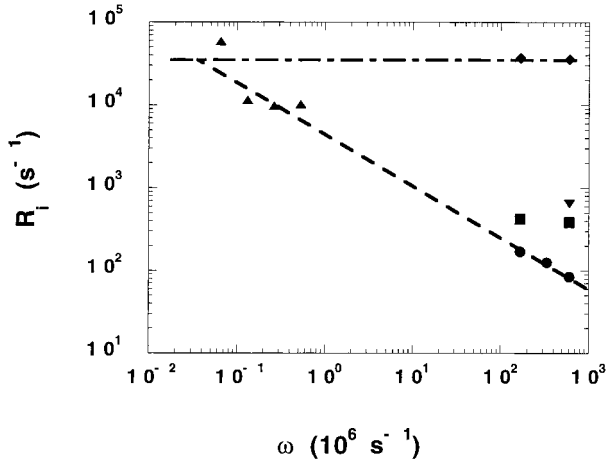

Figure 6. Frequency variation of ^{23}Na relaxation rates measured for aqueous suspensions of Montmorillonite (5%, w/w): (●, R_1; ◆, R_2^f; ■, R_2^s; ▲, $R_{1\rho}^f$; ▼, $R_{1\rho}^s$).

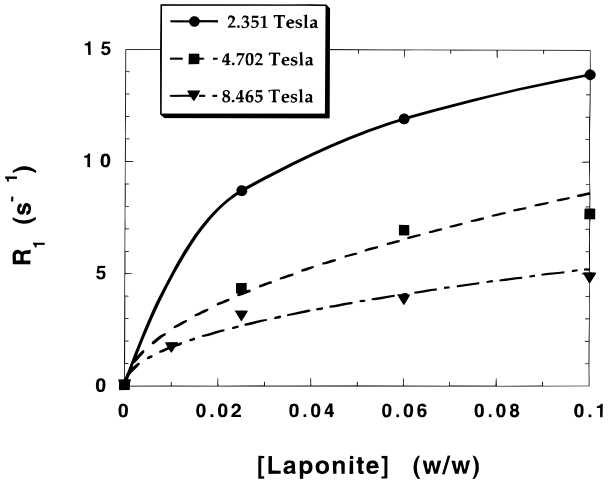

Figure 7. Influence of Laponite concentration on ^{7}Li longitudinal relaxation rate: (●, R_1; ◆, R_2^f; ■, R_2^s; ▲, $R_{1\rho}^f$; ▼, $R_{1\rho}^s$).

counterions in the derivation of the autocorrelation function of the quadrupolar coupling.

In the present study, we focus our comparison on the crossover frequency between the two dynamical regimes detected both on theoretical and experimental spectral densities. Since this crossover frequency is the fingerprint of the size of microdomains containing partially oriented clay particles, these results illustrate the potentiality of nuclear quadrupolar relaxation as a sensitive probe of the spatial extent of orientational order within aqueous clay dispersions.

(B) ^{23}Na Relaxation in Montmorillonite Dispersions. Another check of our model may be performed by increasing the size of the clay particles, in order to enhance the spatial extension of the nematic domains. But before using natural Montmorillonite clay particles to perform such studies, we first investigated the influence of iron on the ^{23}Na relaxation in presence of clays. After adding large amount of iron (10^{-3} M $FeCl_3$) to Laponite suspensions we detected only a weak increase (10%) of the ^{23}Na relaxation rates. Since trivalent Fe^{3+} counterions are highly condensed at the clay surface,[32,33] this result precludes a dominant influence of paramagnetic impurities of natural clays on ^{23}Na relaxation. The strong electrostatic repulsion between condensed Na^+ and Fe^{3+} counterions is certainly responsible for the minimization of the sodium−iron dipolar coupling.

Frequency variation of ^{23}Na counterions in presence of Montmorillonite is shown on Figure 6. The results are quite similar to those of Figure 5 except for the noticeable shift of the crossover frequency down to $\omega \sim (2-4) \times 10^4$ s^{-1}. This 2-order of magnitude shift of the time scale was expected since the persistence length of these Montmorillonite particles, as detected by TEM[5], is about 4000 Å, i.e., 10 times larger than the diameter of the Laponite particles. Figure 6 also displays a somewhat different frequency variation of the spectral densities ($J(\omega) \sim \omega^{-0.6\pm0.2}$), which we cannot explain because of the lack of full MD simulations. Exponent smaller than one are expected to occur only for free diffusion within space of reduced dimensionality ($D < 2$),[28,34] but we expect ionic motion to be very sensitive to strength of the clay/counterion coupling, which varies as a function of the lateral extent of the charged lamellar particles.

(C) ^{7}Li Relaxation in Laponite Dispersions. In order to generalize this study, we also tested another quadrupolar nucleus (^{7}Li) in the presence of Laponite clay. The results (Figure 7) are very similar to those already reported for ^{23}Na, except for

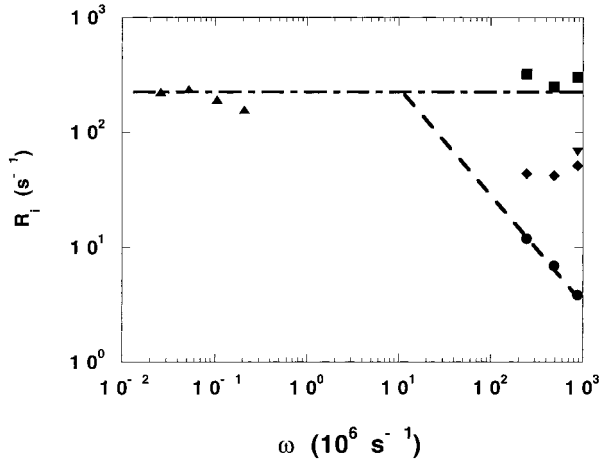

Figure 8. Frequency variation of ^{7}Li relaxation rates measured for aqueous suspensions of Laponite (6%, w/w): (●, R_1; ◆, R_2^f; ■, R_2^s; ▲, $R_{1\rho}^f$; ▼, $R_{1\rho}^s$).

the order of magnitude of the relaxation rates. The ratio between ^{23}Na and ^{7}Li relaxation rates is about 14 ± 2, smaller than the ratio (300) expected from the square of the product of their quadrupolar moment by their antishielding factor.[16] Assuming the organization of the clay particles to be only sensitive to the valency of its neutralizing counterions, various causes may be responsible for that discrepancy: first, the fractions of condensed sodium and lithium counterions are not necessarily the same, because of preferential condensation of the smaller hydrated counterion;[32] secondly, the average electric field gradient felt by both nuclei may differ, because of their different solvation properties; thirdly, the dynamical properties of lithium counterions in the presence of clay may differ from those of sodium due to some specific clay/counterion interactions.

The frequency variation of the relaxation rates may help to distinguish between these possible explanations. The slope shown on Figure 8 (1.0 ± 0.1) is equivalent to that reported for ^{23}Na in presence of Laponite (cf. Figure 5), but the crossover frequency (10^7 s^{-1}) is 5 times larger for lithium than for sodium, while the ratio of their diffusion coefficient is ∼1. This result proves the large influence of the dynamics of quadrupolar nuclei on their relaxation behavior but requires full M.D. simulations in order to be understood.

In any case, because of the decrease of its quadrupolar coupling, ^{7}Li appears to be a probe well suited for relaxation measurements by using field cycling spectrometer,[28,29] filling

the gap between our low field ($T_{1\rho}$) and high field (T_1) measurements.

(D) Time-Scale Limitations. Various time-scale conditions must be fulfilled to extract dynamical information from the frequency variation of the Nuclear Quadrupolar Relaxation rates of $^3/_2$-spin nuclei in heterogeneous systems. These conditions concern: (i) signal detection, (ii) exchange between free and condensed ions, (iii) modulation of quadrupolar coupling, (iv) mobility of adsorbing clay particles, (v) the time scales characterizing the autocorrelation function of the residual quadrupolar coupling and the relaxation of the magnetizations.

First, the dead time of the spectrometer plus the delay before acquisition and the dwell time of the acquisition procedure must be smaller than the longitudinal and transverse relaxation times, otherwise no signal is detected. For ^{23}Na in presence of Montmorillonite and Laponite, this detection condition is not always satisfied by the fast component of the transverse magnetization.

Secondly, in order to record 100% of the NMR signal, the free and condensed counterions must exchange rapidly at the time scale of the relaxation times,[35,36] mixing their magnetization in a single resonance line. Otherwise, condensed counterions will produce a separate very broad resonance line which will not be detected.

Thirdly, no dynamical information will be gained from the frequency variation of the relaxation rates of $^3/_2$-spin nuclei if their quadrupolar coupling is not under slow modulation condition ($\omega\tau_C < 1$).[18−22]

Fourthly, the autocorrelation function of the residual quadrupolar coupling is monitored by ion diffusion within charged interfaces if the clay particles retain their orientation and position for a time longer than the correlation time of the quadrupolar coupling. As recently shown by dynamic light scattering,[37] this condition is satisfied for the smaller Laponite particle, and thus a fortiori for the larger Montmorillonite particle.

Fifthly, this analysis of the relaxation measurements is valid if the correlation time of the residual quadrupolar coupling (τ_C) is much smaller than the longitudinal and transverse relaxation times.[12] This condition is generally satisfied for homogeneous systems; however, for ^{23}Na in the presence of Montmorillonite and because of the long correlation time ($\tau_C \sim 2 \times 10^{-6}$ s) and the small transverse relaxation time ($T_2^f \sim 3 \times 10^{-5}$ s), we reach the upper limit of validity of the present approach.

IV. Conclusions

By comparing the frequency variations of the relaxation rates of ^{23}Na and ^{7}Li in aqueous dispersions of clays of various sizes with the theoretical predictions of ion diffusion and relaxation within heterogeneous media, we demonstrated the potentiality of nuclear quadrupolar relaxation as a sensitive probe of the spatial extent of orientational interfacial order within charged systems.

Acknowledgment. We cordially thank Dr. H. van Damme (CRMD, Orléans, France) for his interest to the progress of this work and for the gift of Montmorillonite sample, Drs. R. Setton (CRMD, Orléans, France), J. C. Leyte (Gorlaeus Laboratory, Leiden, Holland), D. Petit, and J. P. Korb (PMC, Palaiseau, France) for interesting discussions, Drs. J. P. Coutures, D. Massiot, and P. Florian (CRMHT, Orléans, France) for the access to the MSL200 spectrometer, and Région Centre (France) for the purchase of the DSX 100 and 360 spectrometers.

References and Notes

(1) Israelachvili, J. N. *Intermolecular and Surface Forces*; Academic Press: London, 1985.
(2) Lyklema, J. *Fundamentals of Interface and Colloid Science*; Academic Press: London, 1981.
(3) Mourchid, A.; Delville, A.; Lambard, J.; Lécolier, E.; Levitz, P. *Langmuir* **1995**, *11*, 1942.
(4) Ben Ohoud, M.; van Damme, H. *C. R. Acad. Sci. Paris* **1990**, *311*, 665.
(5) Hetzel, F.; Tessier, D.; Jaunet, A. M.; Doner, H. *Clays Clay Miner.* **1994**, *42*, 242.
(6) Urry, D. W.; Trapane, T. L.; Venkatachalam, C. M.; Prasad, K. U. *J. Am. Chem. Soc.* **1986**, *108*, 1448.
(7) Jang, H. M.; Fuerstenau, D. W. *Langmuir* **1987**, *3*, 1114.
(8) Zwetsloot, J. P. H.; Leyte, J. C. *J. Colloid Interface Sci.* **1996**, *181*, 351.
(9) Porion, P.; Faugère, M. P.; Lécolier, E.; Gherardi, B.; Delville, A. *J. Phys. Chem. B* **1998**, *102*, 3477.
(10) Low, P. F. *Soil Sci. Soc. Am. J.* **1980**, *44*, 667.
(11) Thompson, D. W.; Butterworth, J. T. *J. Colloid Interface Sci.* **1992**, *151*, 236.
(12) Abragam, A. *The Principle of Nuclear Magnetism*; Clarendo: Oxford, 1961.
(13) Slichter, C. P. *Principles of Magnetic Resonance*; Springer-Verlag: Berlin, 1978.
(14) Ernst, R. R.; Bodenhausen, G.; Wokaun, A. *Principles of Nuclear Magnetic Resonance in One and Two Dimensions*; Clarendo: Oxford, 1991.
(15) Callaghan, P. T. *Principles of Nuclear Magnetic Resonance Microscopy*; Clarendo: Oxford, 1991.
(16) Hertz, H. G. *Ber. Bunsen-Ges. Phys. Chem.* **1973**, *77*, 531.
(17) Sternheimer, R. M. *Phys. Rev.* **1966**, *146*, 140.
(18) McLachlan, A. D. *Proc. R. Soc. London* **1964**, *A280*, 271.
(19) Hubbard, P. S. *J. Chem. Phys.* **1970**, *53*, 985.
(20) Bull, T. E. *J. Magn. Reson.* **1972**, *8*, 344.
(21) Werbelow, L. G. *J. Chem. Phys.* **1979**, *70*, 5381.
(22) Petit, D.; Korb, J. P. *Phys. Rev. B* **1988**, *37*, 5761.
(23) Blicharski, J. S. *Acta Phys. Pol. A* **1972**, *41*, 223.
(24) Delville, A. *Langmuir* **1991**, *7*, 547.
(25) Delville, A. *J. Phys. Chem.* **1993**, *97*, 9703.
(26) Korb, J. P.; Delville, A.; Demeulenaere, G.; Costa, P.; Jonas, J. *J. Chem. Phys.* **1994**, *101*, 7074.
(27) Delville, A.; Letellier, M. *Langmuir* **1995**, *11*, 1361.
(28) Kimmich, R. *NMR Tomography, Diffusometry, Relaxometry*; Springer-Verlag: Berlin, 1997.
(29) Korb, J. P.; Whaley-Hodges, M.; Bryant, R. G. *Phys. Rev. E* **1997**, *56*, 1934.
(30) Pasquier, V.; Levitz, P.; Delville, A. *J. Phys. Chem.* **1996**, *100*, 10249.
(31) Mitra, P. P.; Sen, P. N.; Schwartz, L. M. *Phys. Rev. Lett.* **1993**, *47*, 8565.
(32) Pellenq, R. J. M.; Caillol, J. M.; Delville, A. *J. Phys. Chem. B* **1997**, *101*, 8584.
(33) Delville, A. *J. Phys. Chem. B* **1999**, *103*, 8296.
(34) Avogadro, A.; Villa, M. *J. Chem. Phys.* **1977**, *66*, 2359.
(35) Woessner, D. E. *J. Chem. Phys.* **1961**, *35*, 41.
(36) Sandström, J. *Dynamic NMR Spectroscopy*; Academic Press: New York, 1982.
(37) Bonn, D.; Tanaka, H.; Wegdam, G.; Kellay, H.; Meunier, J. *Europhys. Lett.* **1999**, *45*, 52.
(38) Levij, M.; De Bleijser, J.; Leyte, J. C. *Chem. Phys. Lett.* **1981**, *83*, 183.
(39) Halle, B.; Wennerström, H.; Piculell, L. *J. Phys. Chem.* **1984**, *88*, 2482.